Supplementary materials

Calcium/aluminum-cored asymmetric bilayer nanoparticles for codelivery of Ziyuglycoside II and PD-L1 siRNA exert anti-breast tumor effects

Methods

Immunofluorescence staining for calreticulin

4T1 breast cancer cells were plated at a density of 2×10^5 cells per well in 6-well plates and cultured overnight at 37℃ in a 5% CO_2 humidified incubator. The cells were assigned to two groups: control group treated with DMSO and ZYII-treated group (5 μg/mL) for further incubation for 4 h. After fixation with 4% PFA and blocking, cells were incubated with anti-calreticulin (CRT) primary antibody (ab2907, 1:500) overnight at 4°C, followed by Alexa Fluor 488 secondary antibody (ab150077, 1:500) for 60 min at room temperature in the dark. Nuclei were stained with DAPI, and images were acquired using a TCS SP8 confocal laser scanning microscope (Leica, Hessian, Germany).

Dynamic light scattering analysis for carrier degradation

For characterization of pH-responsive degradation via dynamic light scattering (DLS), CA/ZYII-siP-c-L was dispersed in an appropriate volume of phosphate-buffered saline (PBS, pH 7.4 and 5.0), respectively, to a final

concentration of 0.3 mg/mL, calculated based on the ZYII loading content. The hydrodynamic diameter and polydispersity index (PDI) of the nanoparticles were monitored using a Malvern Zetasizer (ZEN3690, UK) at pre-determined time points (0, 4, 12, and 24 h), with three replicate measurements performed for each sample.

Results

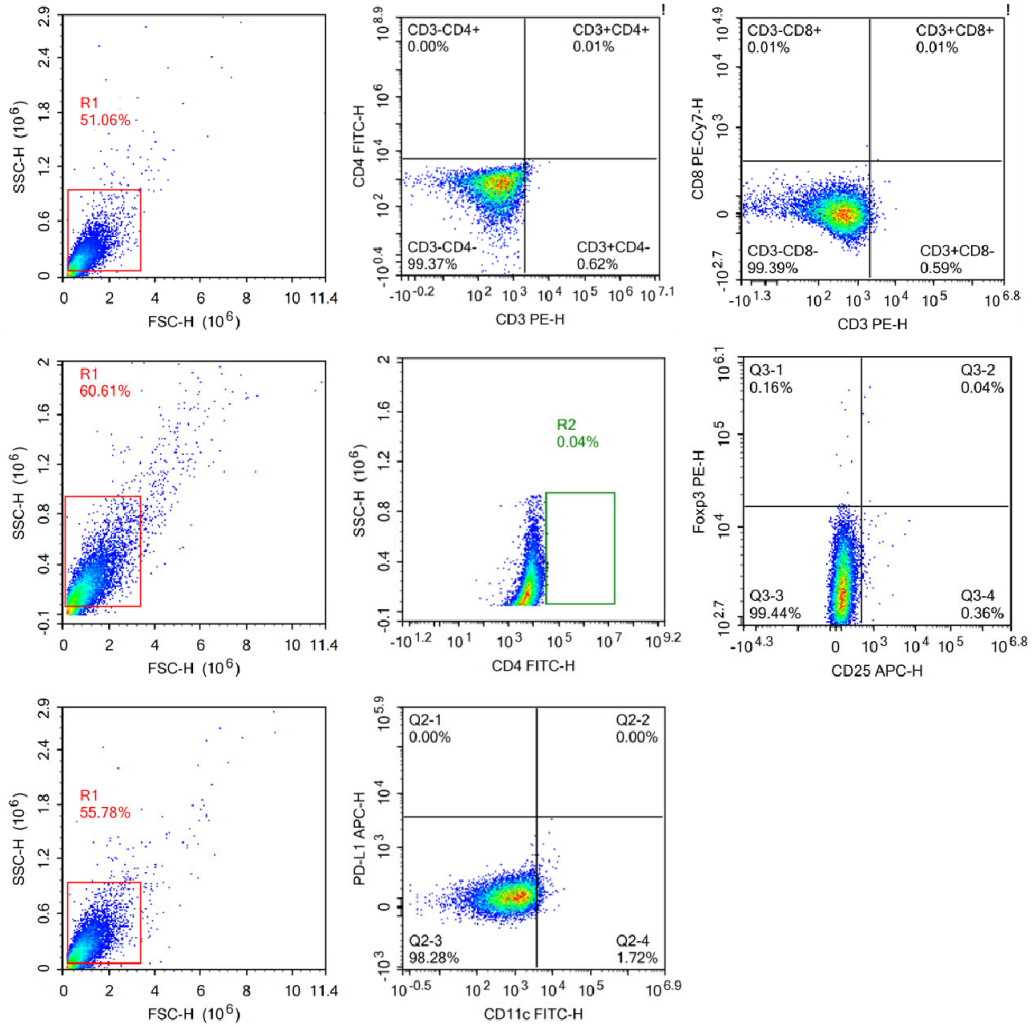


Figure S1. Flow cytometric gating and fluorescence compensation validation for the panels.

CRT exposure induction

As shown in Figure S1, weak CRT surface fluorescence was observed in the DMSO-treated group. ZYII solution (5 μg/mL) induced significant cell surface CRT aggregation with marked green fluorescence enhancement, indicating ZYII is effective for inducing CRT exposure.

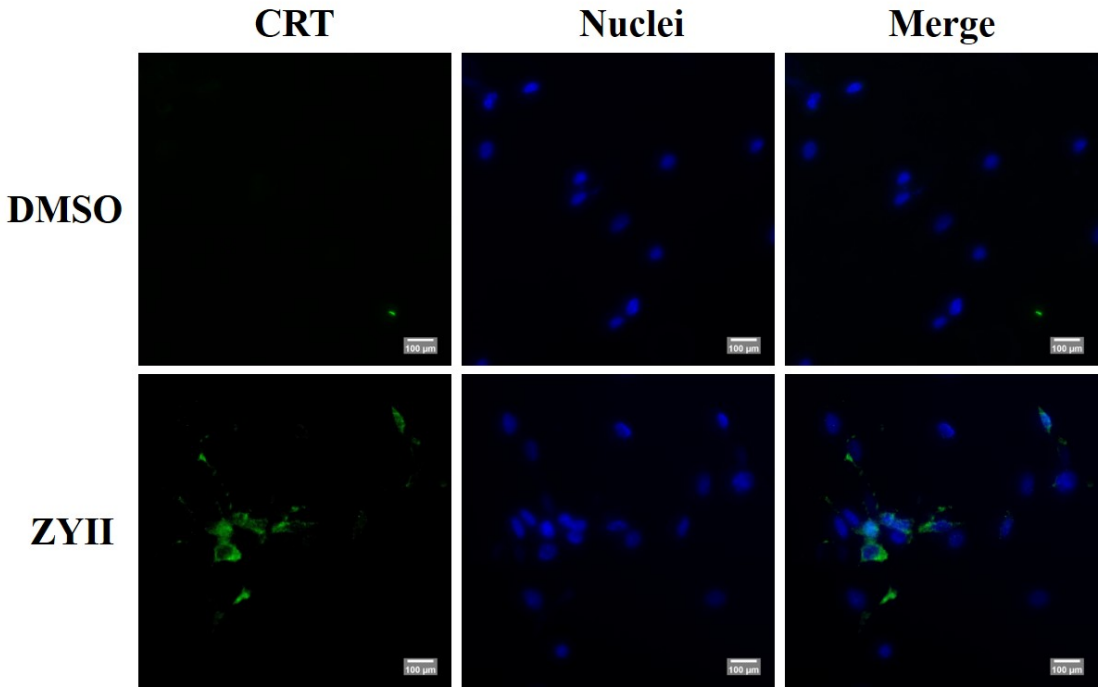


Figure S2. CRT exposure induction from DMSO-treated and ZYII-treated. 4T1 cells (Bar equals 100 μm).

DLS-evaluated degradation

As shown in Table S1, CA/ZYII-siP-c-L exhibited distinct pH-responsive structural changes over 24 h. At pH 5.0, the hydrodynamic diameter first slightly swelled at 4 h, then decreased significantly to 65 nm at 24 h, with a transient increase in PDI at 12 h reflecting heterogeneous degradation. In

contrast, at pH 7.4, both the hydrodynamic diameter and PDI remained stable throughout the incubation period, with only a moderate reduction in diameter by 24 h. These results confirm that the formulation undergoes acid-induced structural degradation at pH 5.0 while remaining stable at physiological pH, thereby driving its pH-dependent release behavior.

Table S1. pH-dependent changes in hydrodynamic diameter and PDI of CA/ZYII-siP-c-L.

Time (h)	pH 5.0		pH 7.4	
	Size (nm)±SD	PDI±SD	Size (nm)±SD	PDI±SD
0	185.7±2.1	0.22±0.02	185.7±2.1	0.22±0.02
4	195.5±3.5	0.24±0.03	182.1±2.6	0.21±0.02
12	140.3±4.2	0.35±0.03	175.8±3.1	0.23±0.02
24	65.0±2.8	0.23±0.02	145.0±2.9	0.24±0.02

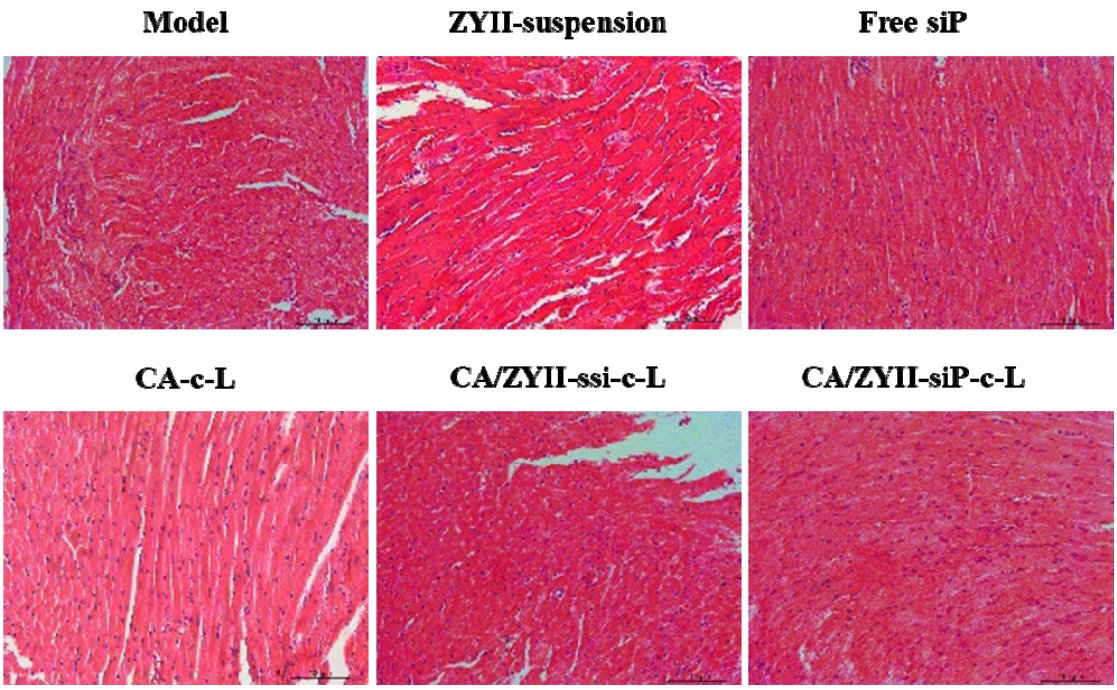


Figure S3. H&E staining of heart tissues from all treatment groups.

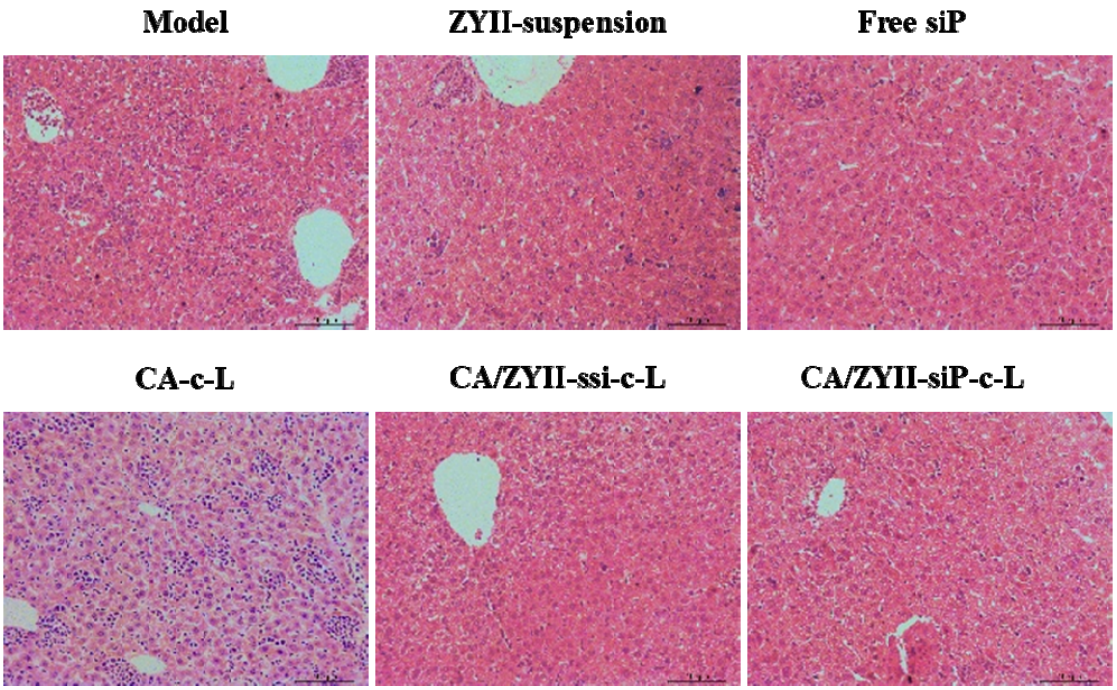


Figure S4. H&E staining of liver tissues from all treatment groups.

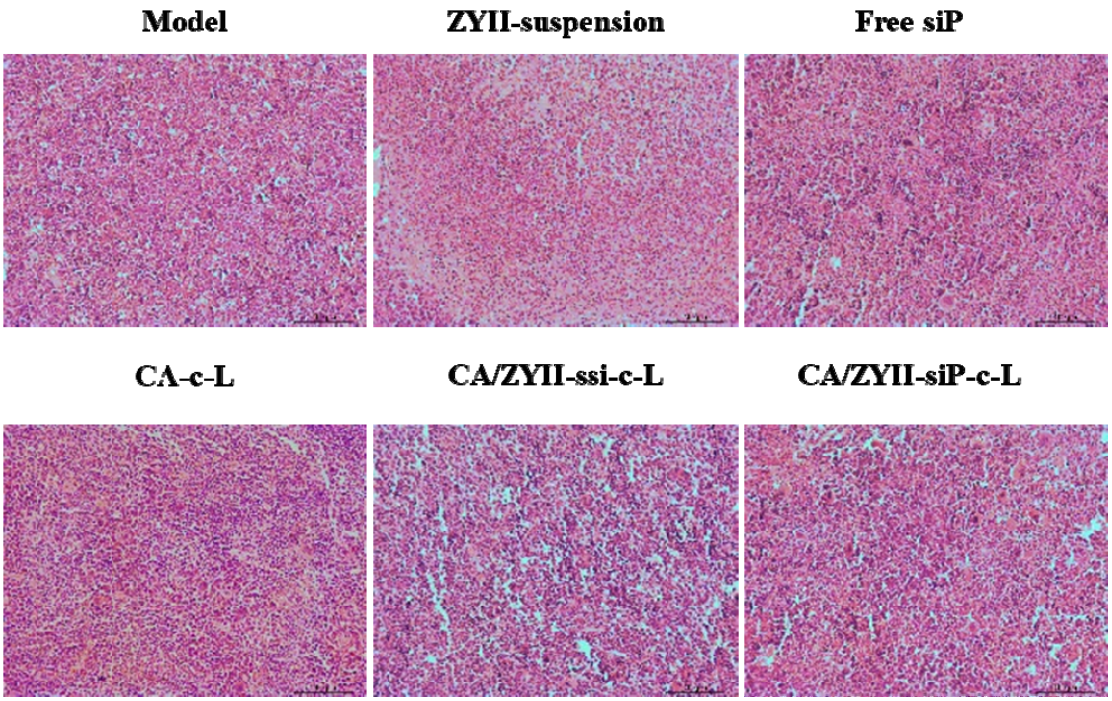


Figure S5. H&E staining of spleen tissues from all treatment groups.

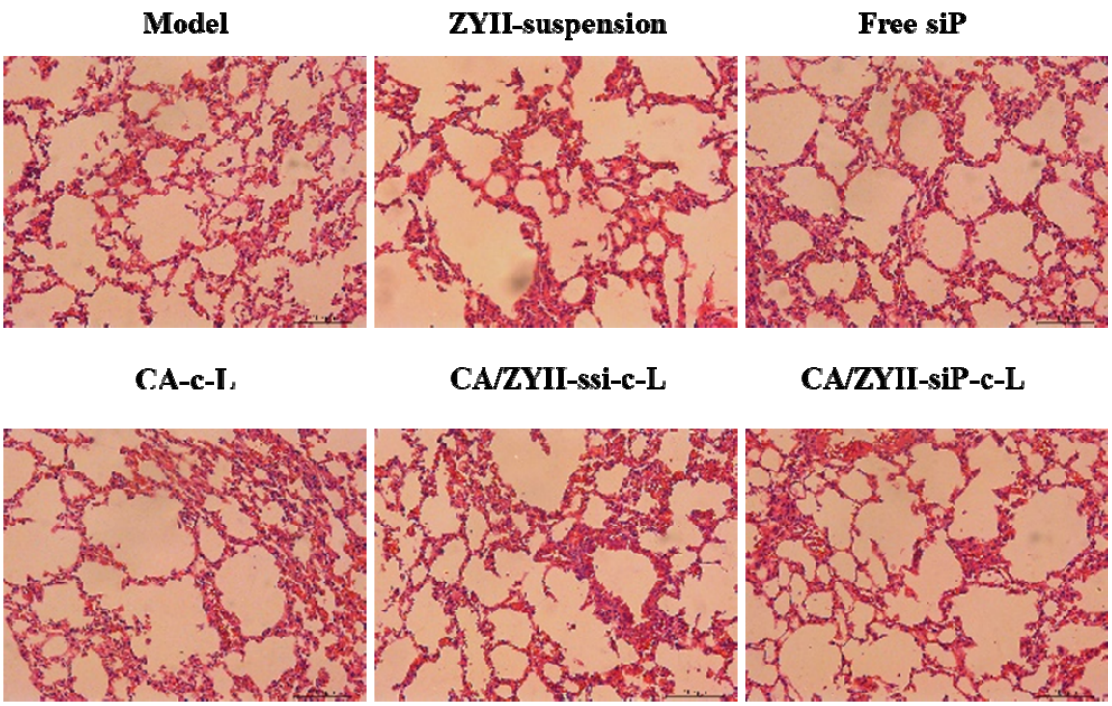


Figure S6. H&E staining of lung tissues from all treatment groups.

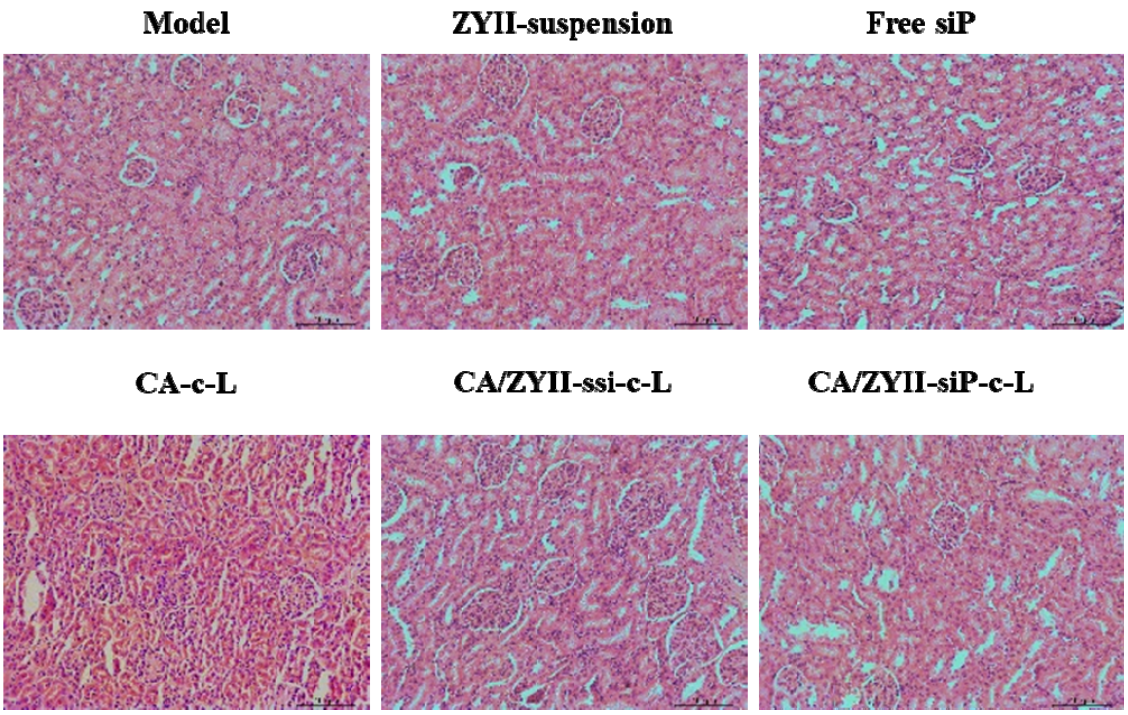


Figure S7. H&E staining of kidney tissues from all treatment groups.

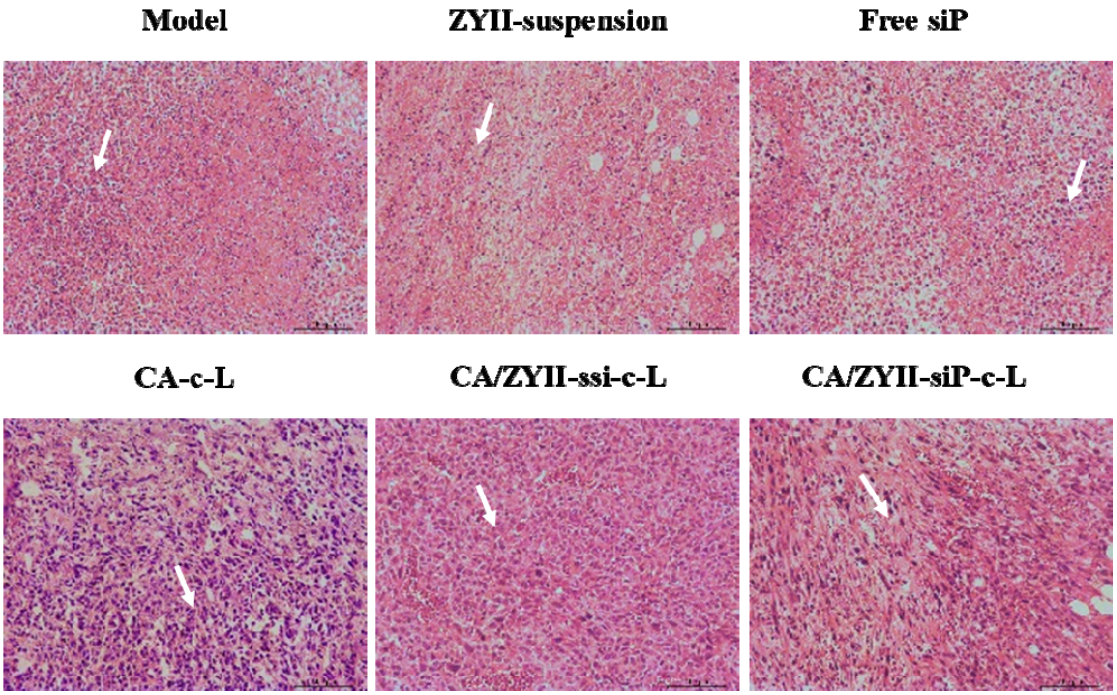


Figure S8. H&E staining of tumor tissues from all treatment groups; arrows indicate the key histopathological change areas in the tumor tissues of each group.